

## A REGULARIZATION METHOD FOR THE NUMERICAL SOLUTION OF SHALLOW WATER EQUATIONS

Tatiana G. Elizarova\* and Jean-Claude Lengrand†

\*Institute for Mathematical Modeling  
Miusskaya sq. 4a, 125047 Moscow, Russia  
e-mail: telizar@yahoo.com

†CNRS/ICARE  
1C, av. de la recherche scientifique, 45071 Orléans cedex 2  
e-mail: jc.lengrand@orange.fr

**Key words:** regularization, quasi-gasdynamics system, quasi-hydrodynamic system, shallow water equations, hydraulic jump

**Abstract.** *Two variants of regularized shallow water equations are proposed based on two variants of regularized Navier-Stokes equations, namely quasi-gasdynamics and quasi-hydrodynamic equations. The regularization allows implementing efficient finite-difference algorithms for the numerical solution, where the stability of calculations is provided by the included regularization terms. The domain of validity of both variants is tested on the problem of a hydraulic jump.*

## 1 INTRODUCTION

Based on a number of hypotheses, the inviscid flow of a liquid can be treated by the so-called *Shallow Water Equations*. This approach has been widely used in the mathematical description of a number of problems [1, 2].

The shallow water equations are closely related to the gasdynamic equations: they can be derived formally from the barotropic approximation of Euler equations. It is the reason why numerical algorithms for solving the shallow water equations are often based on numerical methods for Euler equations.

Recently an efficient numerical algorithm for calculations of viscous and inviscid compressible gas flows has been developed. It is based on a special form of regularization in the Navier-Stokes (NS) equation system that includes additional dissipative terms. The latter have the form of second-order space derivatives in factor of a small parameter  $\tau$ . These new equations were called quasi-gasdynamic (QGD) and quasi-hydrodynamic (QHD) equations [3, 4, 5]. The numerical algorithms based on QGD and QHD equations have shown their efficiency in a number of numerical computations for various problems of fluid dynamics.

In this paper the QGD and QHD additional terms are modified by the same transformation that changes Euler equations into shallow water equations and added to the latter. *Regularized Shallow Water* (RSW) equations are thus obtained. The corresponding numerical methods are proposed and tested on the problem of hydraulic jump.

## 2 SHALLOW WATER EQUATIONS AND THE BAROTROPIC APPROXIMATION OF EULER EQUATIONS

Euler equations in index form writes

$$\frac{\partial \rho}{\partial t} + \frac{\partial(\rho u_i)}{\partial x_i} = 0, \quad (1)$$

$$\frac{\partial(\rho u_i)}{\partial t} + \frac{\partial}{\partial x_j}(\rho u_j u_i) + \frac{\partial p}{\partial x_i} = \rho f_i, \quad (2)$$

$$\frac{\partial E}{\partial t} + \frac{\partial}{\partial x_i} u_i (E + p) = \rho u_i f_i. \quad (3)$$

The unknown in Eqs (1)-(3) are the gas density  $\rho(x_i, t)$ , the gas velocity  $u_i(x_j, t)$  and the pressure  $p(x_i, t)$ . The total energy  $E(x_i, t)$  per unit-volume is related to these unknown. For a dilute gas with constant specific heats, we have  $E = (\rho u_i u_i / 2) + (p / (\gamma - 1))$ , where  $\gamma$  is the ratio of specific heats (adiabatic exponent).  $f_i$  is an external volume force per unit-mass.

The barotropic approximation consists in reducing the system, assuming that pressure depends only on density

$$p = p(\rho). \quad (4)$$

Assuming again the gas to be dilute with constant specific heats and its evolution to be adiabatic and reversible (i.e. isentropic), we have

$$\frac{dp}{p} = \gamma \frac{d\rho}{\rho}. \quad (5)$$

The shallow water equations for a flow over a plane horizontal bottom write

$$\frac{\partial h}{\partial t} + \frac{\partial(u_i h)}{\partial x_i} = 0, \quad (6)$$

$$\frac{\partial(hu_i)}{\partial t} + \frac{\partial(hu_j u_i)}{\partial x_j} + \frac{\partial}{\partial x_i} \left[ \frac{gh^2}{2} \right] = 0. \quad (7)$$

Considering Euler equations in the absence of external volume force ( $f_i = 0$ ), equations (1) and (2) can be formally transformed into equations (6) and (7) if the gas density  $\rho$  is replaced by  $h$ , and the pressure  $p$  is replaced by  $gh^2/2$ . This replacement forces a relationship between the variations of  $\rho$  and  $p$ :

$$\frac{dp}{p} = 2 \frac{d\rho}{\rho}, \quad (8)$$

consistent with  $\gamma = 2$  in Euler equations. The formal change

$$\rho \rightarrow h, p \rightarrow gh^2/2, \gamma \rightarrow 2 \quad (9)$$

will be applied to the regularization terms of QGD and QHD equations.

### 3 REGULARIZED SHALLOW WATER EQUATIONS

A detailed presentation of QGD and QHD equations can be found in [3]. In the absence of external volume forces, both systems have the general form

$$\frac{\partial \rho}{\partial t} + \frac{\partial j_{mi}}{\partial x_i} = 0, \quad (10)$$

$$\frac{\partial(\rho u_i)}{\partial t} + \frac{\partial}{\partial x_j} (j_{mj} u_i) + \frac{\partial p}{\partial x_i} = \frac{\partial}{\partial x_j} \Pi_{ji}, \quad (11)$$

$$\frac{\partial E}{\partial t} + \frac{\partial}{\partial x_i} j_{mi} \frac{E+p}{\rho} + \frac{\partial}{\partial x_i} q_i = \frac{\partial}{\partial x_j} \Pi_{ji} u_j. \quad (12)$$

Here  $\Pi_{ij}$  and  $q_i$  are the shear-stress tensor and the heat flux vector, respectively.  $j_m$  is a modified mass flux vector, that differs from  $\rho u$  by a small quantity

$$j_{mi} = \rho(u_i - w_i) \quad (13)$$

with 
$$w_i = \frac{\tau}{p} \left( \frac{\partial}{\partial x_j} (\rho u_j u_i) + \frac{\partial}{\partial x_i} p \right) \quad (\text{QGD}) \quad (14)$$

or 
$$w_i = \frac{\tau}{p} \left( \rho u_i \frac{\partial u_j}{\partial x_j} + \frac{\partial}{\partial x_i} p \right) \quad (\text{QHD}). \quad (15)$$

Similarly  $\Pi$  is a modified shear-stress tensor, equal to the Navier-Stokes (NS) one plus an additional term.

The additional terms in both QGD and QHD systems involve a small parameter  $\tau$  that has the dimension of a time. According to the application,  $\tau$  has a physical meaning (molecular

relaxation time in rarefied gas flows, time-averaging parameter in turbulent flows) or can be regarded as purely numerical, the additional terms acting as regularizing terms.

When solving Euler equations for supersonic gas flows, the NS terms  $\Pi_{ij}$  and  $q_i$  can be kept as regularizing terms if the coefficients of viscosity  $\mu$  and thermal conductivity  $\kappa$  are expressed in terms of  $\tau$ , e.g.,  $\mu = p\tau$ . It was shown that the regularizing additions have a dissipative nature. For stationary flows they have the order of  $O(\tau^2)$ . A wide range of Euler flow calculations with QGD and QHD models can be found in, e.g., [3] and [5] and citations therein. Recent results are presented in [6] and [7]. The associated algorithms are characterized by the accuracy of the mathematical solution for oscillating flows, the natural adaptation to unstructured space grids and the possibility of efficient implementation on multiprocessor computers. The barotropic approximations of the QGD and QHD equations were studied recently in [11] and [12].

Let us consider the barotropic approximation of Eqs (10)-(12). By applying the formal transformation (9), one obtains two variants of the regularized shallow water equation systems: RSW1 based on the QGD approach and RSW2 based on the QHD approach.

We will apply these equations to a hydraulic jump and we restrict here to a 1D flow over a plane horizontal bottom.

RSW1 equations are obtained starting from Eqs 5.51 and 5.52 of [3], applied to a 1D flow:

$$\frac{\partial \rho}{\partial t} + \frac{\partial(\rho u)}{\partial x} = \frac{\partial(\rho w)}{\partial x}, \quad (16)$$

$$\frac{\partial(\rho u)}{\partial t} + \frac{\partial(\rho u^2)}{\partial x} + \frac{\partial p}{\partial x} = \frac{\partial(\rho u w)}{\partial x} + \frac{\partial \Pi}{\partial x}, \text{ with} \quad (17)$$

$$w = \frac{\tau}{\rho} \times \frac{\partial(\rho u^2 + p)}{\partial x}, \Pi = \frac{4}{3} \mu \frac{\partial u}{\partial x} + u\tau \left( \rho u \frac{\partial u}{\partial x} + \frac{\partial p}{\partial x} \right) + \tau \left( u \frac{\partial p}{\partial x} + \gamma p \frac{\partial u}{\partial x} \right) \text{ and } \mu = \tau p. \quad (18)$$

Replacing  $\rho, p$  and  $\gamma$  by  $h, gh^2/2$  and  $2$ , respectively, one obtains RSW1 equations:

$$\frac{\partial h}{\partial t} + \frac{\partial(hu)}{\partial x} = \frac{\partial(hw)}{\partial x}, \quad (19)$$

$$\frac{\partial(hu)}{\partial t} + \frac{\partial(u^2 h)}{\partial x} + \frac{\partial}{\partial x} \left[ \frac{gh^2}{2} \right] = \frac{\partial(huw)}{\partial x} + \frac{\partial \Pi}{\partial x}, \quad (20)$$

where  $w = \frac{\tau}{h} \times \frac{\partial(hu^2 + gh^2/2)}{\partial x}$  and  $\Pi = \tau gh \left[ \left( \frac{5}{3} h + \frac{u^2}{g} \right) \frac{\partial u}{\partial x} + 2u \frac{\partial h}{\partial x} \right]$ . (21)

RSW2 equations differ by the regularizing right-hand terms:

$$\frac{\partial h}{\partial t} + \frac{\partial(hu)}{\partial x} = \frac{\partial(hw)}{\partial x}, \quad (22)$$

$$\frac{\partial(hu)}{\partial t} + \frac{\partial(u^2 h)}{\partial x} + \frac{\partial}{\partial x} \left[ \frac{gh^2}{2} \right] = 2 \frac{\partial(huw)}{\partial x} + \frac{\partial \Pi}{\partial x}, \quad (23)$$

where  $w = \tau \left( u \frac{\partial u}{\partial x} + g \frac{\partial h}{\partial x} \right)$  and  $\Pi = \frac{4}{3} \mu \frac{\partial u}{\partial x}$ . (24)

The last term in the right-hand side of Eq.(23) looks like a usual viscous term. However, the physical viscosity  $\mu$  is replaced by  $\tau p \rightarrow \tau gh^2 / 2$ . This system (without the NS-like term) has been used in [10] to compute the 1D time evolution of an initial level difference as, i.e. after a dam break.

## 4 NUMERICAL TEST-CASE: HYDRAULIC JUMP

### 4.1 Physical problem and analytic solution

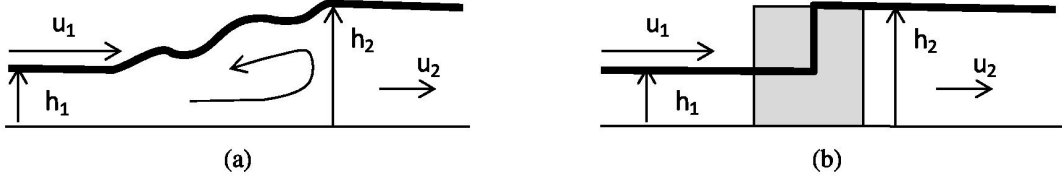


Fig. 1: Hydraulic jump

As a test-case, we treat the 1D flow of an inviscid liquid of density  $\rho$ , in a uniform gravity field of intensity  $g$ . The velocity  $u$  is considered as uniform in a given section. The abscissa  $x$  refers to the flow direction. The particular problem treated is the hydraulic jump, for which an analytic solution exists.

A hydraulic jump is a sudden change in the height  $h$  and velocity  $u$  of the flow. Fig. 1a is a schematic view of the physical phenomenon. A 1D approach is not suitable to describe what happens actually. However, a 1D approach is sufficient to express the conservation laws and to relate conditions upstream and downstream of the jump, referred to as (1) and (2), respectively. The problem is simplified as in Fig. 1b.

The relation between conditions (1) and (2) is obtained by applying mass-conservation

$$h_1 u_1 = h_2 u_2 \quad (25)$$

and the conservation of momentum in the flow direction on the rectangle of height  $h_2$  between sections (1) and (2). We neglect friction forces on the bottom and on the atmosphere. Thus the only forces are pressure forces. The pressure distribution is linear (i.e. hydrostatic) in a given section. Let  $p_0$  denote the atmospheric pressure. Reasoning per unit-width, we obtain the pressure forces  $\left(p_0 + \rho g \frac{h_1}{2}\right)h_1 + p_0(h_2 - h_1)$  and  $\left(p_0 + \rho g \frac{h_2}{2}\right)h_2$  in the positive and negative directions, respectively. Their difference is equal to the increase of momentum flux  $\rho u_1 h_1 (u_2 - u_1) = \rho u_1^2 h_1 \left(\frac{h_1}{h_2} - 1\right)$ . Thus

$$\left(p_0 + \rho g \frac{h_1}{2}\right)h_1 + p_0(h_2 - h_1) - \left(p_0 + \rho g \frac{h_2}{2}\right)h_2 = \rho u_1^2 h_1 \left(\frac{h_1}{h_2} - 1\right)$$

which simplifies as

$$u_1 = \left(g \frac{h_1 + h_2}{2} \times \frac{h_2}{h_1}\right)^{1/2}. \quad (26)$$

We introduce the Froude number, which is the ratio of flow velocity to the velocity of surface waves

$$\text{Fr}_1 = \frac{u_1}{(gh_1)^{1/2}} \quad \text{and} \quad \text{Fr}_2 = \frac{u_2}{(gh_2)^{1/2}} \quad (27)$$

and Eq.(26) becomes

$$\text{Fr}_1 = \frac{u_1}{(g h_1)^{1/2}} = \left( \frac{1}{2} \left( 1 + \frac{h_2}{h_1} \right) \frac{h_2}{h_1} \right)^{1/2}. \quad (28)$$

If the upstream Froude number is known, we obtain the height ratio  $h_2 / h_1$  as the solution of the second order equation  $X^2 + X - 2\text{Fr}_1^2 = 0$ , that has only one positive solution

$$\frac{h_2}{h_1} = \frac{1}{2} \left( -1 + \left( 1 + 8\text{Fr}_1^2 \right)^{1/2} \right). \quad (29)$$

Then we deduce  $h_2 = h_1 \times \frac{h_2}{h_1}$ ,  $u_2 = \frac{h_1 u_1}{h_2}$ ,  $\text{Fr}_2 = \frac{u_2}{(g h_2)^{1/2}}$ .

$h_2 / h_1$  is an increasing function of  $\text{Fr}_1$ , with the limiting case  $h_1 = h_2$  for  $\text{Fr}_1 = 1$ .

The hydraulic jump equations are perfectly symmetric in (1) and (2). However the second law of thermodynamics requires that the hydraulic energy (specific head) does not increase. Therefore  $(h_1 + u_1^2 / 2) - (h_2 + u_2^2 / 2)$  must be not negative. This requires  $\text{Fr}_1 \geq 1$  (torrential regime) and therefore  $h_2 \geq h_1, u_2 \leq u_1, \text{Fr}_2 \leq 1$  (fluvial regime). A hydraulic jump is equivalent to a normal shock in a 1D gas flow that makes the flow switch from supersonic (Mach number  $>1$ ) to subsonic (Mach number  $<1$ ).

The hydraulic jump is a rather severe test-case, due to the discontinuity.

## 4.2 Numerical algorithm

As was done for QGD and QHD equations, the RSW1 and RSW2 equations were solved by an explicit finite-volume approach, using a central finite-difference approximation for all terms, including the convective ones.

The regularizing terms are favorable to the stability of the solution. They act as artificial dissipation and depend on a single parameter  $\tau$  which is taken locally as

$$\tau(x, t) = \alpha \Delta x / c(x, t), \quad (30)$$

where  $c(x, t) = (g h(x, t))^{1/2}$  is the local speed of surface waves and  $\Delta x$  is the computational grid step. The value of  $\alpha$  must ensure stability, while keeping the results close to the exact solution.

The time step was taken from the Courant stability condition

$$\Delta t = \beta \min(\Delta x / c(x, t)), \quad (31)$$

where the minimum is calculated over all grid points at a given time. The constant  $\beta$  has to be adjusted to ensure stability. Based on expression (31),  $\Delta t$  is readjusted at each time step and becomes constant when convergence is approached. However for the present problem, the maximal value of  $h$  at convergence is  $h = h_2$ . Therefore, we take

$$\Delta t = \beta \times (\Delta x / (g h_2)^{1/2}) \quad (32)$$

and do not readjust it during the calculation.

A parametric study was carried out to determine the domain of convergence of the algorithm in terms of  $\alpha$  and  $\beta$  for different values of  $\text{Fr}_1$ , and to check the correctness of the numerical solution, compared with the analytical one, schematized in Fig.1b.

The acceleration of gravity was taken equal to  $9.81 \text{ m}\cdot\text{s}^{-2}$ .  $h_1$  was taken arbitrarily equal to 1 m. The values of  $u_1$ ,  $h_1$ ,  $u_2$ ,  $h_2$  were calculated analytically and used to prescribe the boundary conditions. The initial conditions were characterized by a smooth variation of  $h$  from  $h_1$  at input to  $h_2$  at output and the corresponding value  $u = (h_1 u_1) / h$ .

Unless otherwise specified, the computational domain had a length  $L = 100\text{m}$  and was divided into  $N = 500$  intervals of size  $\Delta x = 0.2\text{m}$ . The calculations were stopped at a predefined maximal physical time. Convergence was monitored by recording the adimensional residues

$$\text{res}_{\text{avg}} = \frac{1}{N-1} \sum_{i=1}^{N-1} \left| \frac{u_i^{j+1} - u_i^j}{u_i^j} \right| \text{ and } \text{res}_{\text{max}} = \max_{i=0}^N \left| \frac{u_i^{j+1} - u_i^j}{u_i^j} \right|. \quad (33)$$

The calculations were carried out on a personal computer. The CPU time depends directly on the value of  $\beta$ . It is approximately inversely proportional to  $\beta$ .

The length of the computational domain was much larger than the jump thickness. Physically, the position of the jump in the computational domain is undetermined. Therefore, the profiles can be arbitrarily translated along the  $x$ -axis. Their exact position is not significant. However, in the present figures, their position is indicated as obtained by the calculation.

When the calculations converged, the final residues were very small, probably governed by the computer precision, i.e. the final state was perfectly steady.

### 4.3 Results for RSW1

Computations were carried out for the first variant of RSW equations (RSW1). Hydraulic jumps were successfully calculated with

$$\text{Fr}_1 = 1.1, h_1 = 1\text{m}, u_1 = 3.445\text{m/s}, h_2 = 1.134\text{m}, u_2 = 3.038\text{m/s}$$

$$\text{Fr}_1 = 2, h_1 = 1\text{m}, u_1 = 6.264\text{m/s}, h_2 = 2.372\text{m}, u_2 = 2.641\text{m/s}$$

$$\text{Fr}_1 = 5, h_1 = 1\text{m}, u_1 = 15.66\text{m/s}, h_2 = 6.589\text{m}, u_2 = 2.377\text{m/s}$$

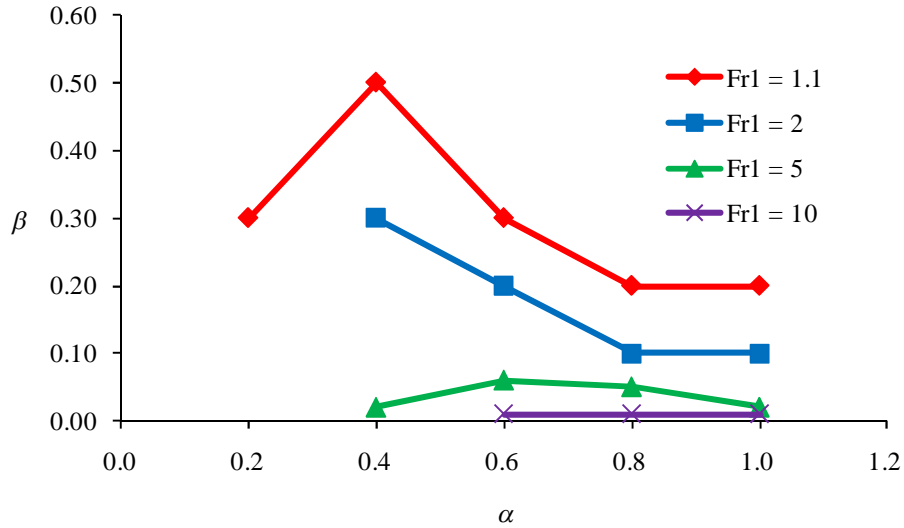
$$\text{Fr}_1 = 10, h_1 = 1\text{m}, u_1 = 31.32\text{m/s}, h_2 = 13.65\text{m}, u_2 = 2.294\text{m/s}.$$

For each test-case, different values of  $\alpha$  were used. For a given  $\alpha$ , different runs with increasing values of  $\beta$  were computed until divergence (Table 1). The highest acceptable value of  $\beta$  was retained and the corresponding line appears in bold in Table 1. The highest admissible value of  $\beta$  is plotted in Fig. 2 as a function of  $\alpha$  and  $\text{Fr}_1$ .

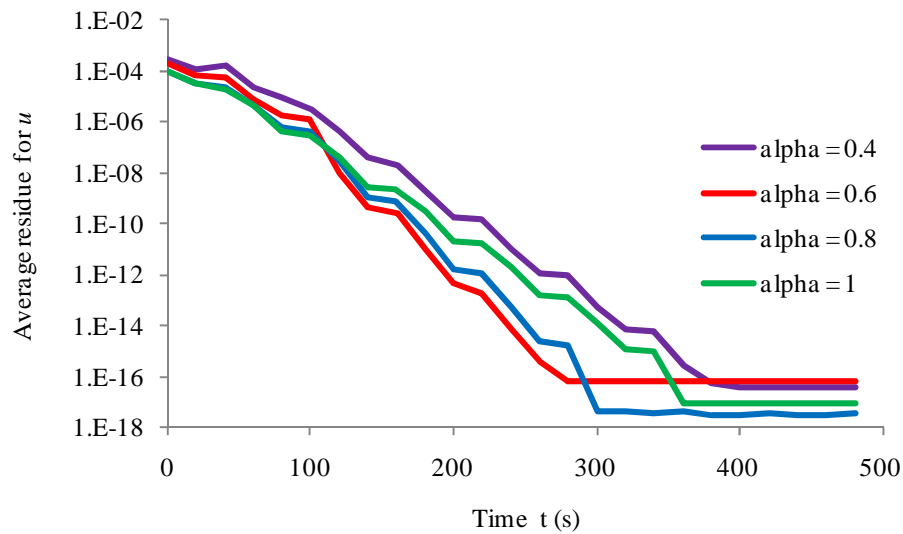
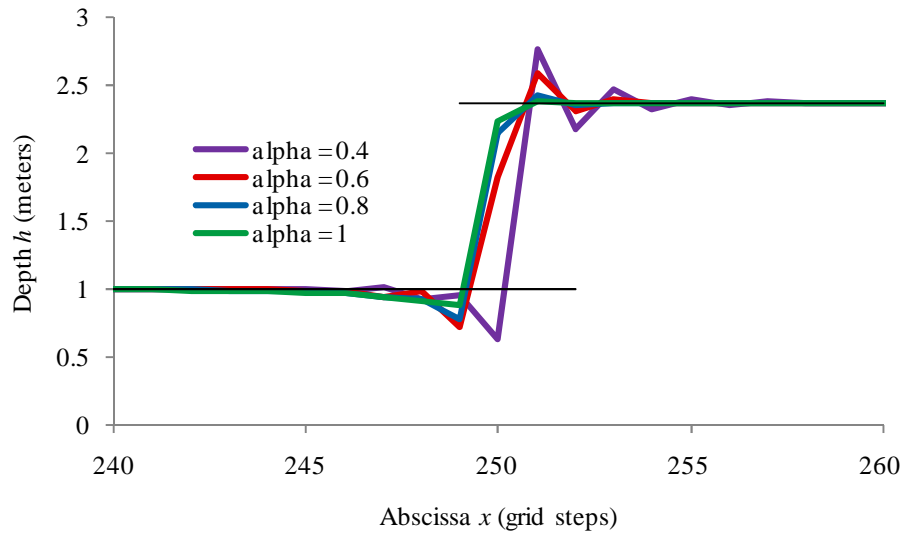
Only the results obtained for  $\text{Fr}_1 = 2$  and  $\text{Fr}_1 = 10$  will be discussed here.

run	$Fr_1$	$\alpha$	$\beta$	$\Delta t$ (s)	$t_{\max}$ (s)	$res_{\text{avg}}$	$res_{\text{max}}$	CPU (s)
<b>RSW1-01</b>	<b>1.1</b>	<b>0.20</b>	<b>0.30</b>	<b>1.80E-02</b>	<b>1500</b>	<b>6.7E-17</b>	<b>1.0E-15</b>	<b>6.8</b>
RSW1-02	1.1	0.40	0.30	1.80E-02	1500	7.9E-18	2.2E-15	6.7
<b>RSW1-03</b>	<b>1.1</b>	<b>0.40</b>	<b>0.50</b>	<b>3.00E-02</b>	<b>1500</b>	<b>1.9E-16</b>	<b>1.0E-15</b>	<b>4.3</b>
<b>RSW1-04</b>	<b>1.1</b>	<b>0.60</b>	<b>0.30</b>	<b>1.80E-02</b>	<b>1500</b>	<b>1.9E-17</b>	<b>1.4E-15</b>	<b>6.4</b>
<b>RSW1-05</b>	<b>1.1</b>	<b>0.80</b>	<b>0.20</b>	<b>1.20E-02</b>	<b>1500</b>	<b>2.3E-17</b>	<b>3.9E-15</b>	<b>10.7</b>
<b>RSW1-06</b>	<b>1.1</b>	<b>1.00</b>	<b>0.20</b>	<b>1.20E-02</b>	<b>1500</b>	<b>3.5E-17</b>	<b>3.5E-15</b>	<b>10.4</b>
<b>RSW1-10</b>	<b>2.0</b>	<b>0.40</b>	<b>0.30</b>	<b>1.24E-02</b>	<b>500</b>	<b>3.7E-17</b>	<b>8.5E-15</b>	<b>3.1</b>
<b>RSW1-09</b>	<b>2.0</b>	<b>0.60</b>	<b>0.20</b>	<b>8.29E-03</b>	<b>500</b>	<b>6.8E-17</b>	<b>1.7E-14</b>	<b>4.8</b>
<b>RSW1-08</b>	<b>2.0</b>	<b>0.80</b>	<b>0.10</b>	<b>4.15E-03</b>	<b>500</b>	<b>3.0E-18</b>	<b>1.0E-15</b>	<b>9.4</b>
<b>RSW1-07</b>	<b>2.0</b>	<b>1.00</b>	<b>0.10</b>	<b>4.15E-03</b>	<b>500</b>	<b>9.7E-18</b>	<b>3.0E-15</b>	<b>9.5</b>
<b>RSW1-14</b>	<b>5.0</b>	<b>0.40</b>	<b>0.02</b>	<b>4.98E-04</b>	<b>500</b>	<b>2.6E-16</b>	<b>7.0E-14</b>	<b>76.1</b>
<b>RSW1-13</b>	<b>5.0</b>	<b>0.60</b>	<b>0.06</b>	<b>1.49E-03</b>	<b>200</b>	<b>4.2E-17</b>	<b>1.2E-14</b>	<b>10.6</b>
<b>RSW1-12</b>	<b>5.0</b>	<b>0.80</b>	<b>0.05</b>	<b>1.24E-03</b>	<b>250</b>	<b>9.7E-17</b>	<b>3.2E-14</b>	<b>15.9</b>
<b>RSW1-11</b>	<b>5.0</b>	<b>1.00</b>	<b>0.02</b>	<b>4.98E-04</b>	<b>200</b>	<b>8.4E-17</b>	<b>2.3E-14</b>	<b>32.5</b>
<b>RSW1-17</b>	<b>10.0</b>	<b>0.60</b>	<b>0.01</b>	<b>1.73E-04</b>	<b>250</b>	<b>2.6E-15</b>	<b>5.5E-13</b>	<b>119.7</b>
<b>RSW1-16</b>	<b>10.0</b>	<b>0.80</b>	<b>0.01</b>	<b>1.73E-04</b>	<b>250</b>	<b>6.4E-16</b>	<b>2.0E-13</b>	<b>114.1</b>
<b>RSW1-15</b>	<b>10.0</b>	<b>1.00</b>	<b>0.01</b>	<b>1.73E-04</b>	<b>250</b>	<b>6.3E-16</b>	<b>2.5E-13</b>	<b>114.6</b>
RSW1-18	10.0	0.60	0.01	1.73E-04	250	5.6E-15	1.7E-12	112.8
RSW1-19	10.0	0.60	0.01	1.73E-04	400	9.8E-11	1.1E-08	180.0

Table 1: Summary of runs with RSW1

Fig.2: Maximal admissible value of  $\beta$  as a function of  $\alpha$  and  $Fr_1$  (RSW1)

The convergence history and the spatial distribution of depth  $h$  for  $Fr_1 = 2$  are plotted in Figs.3 and 4, respectively. All grid points in the vicinity of the jump have been plotted. The jump is very stiff (1-2 grid steps) and accompanied by oscillations that decrease with increasing  $\alpha$ .

Fig.3: Convergence history for  $Fr_1 = 2$  (RSW1)Fig.4: Distribution of depth  $h$  for  $Fr_1 = 2$  (RSW1)

The convergence history and the spatial distribution of depth  $h$  for  $Fr_1 = 10$  are plotted in Figs.5 and 6, respectively. The choice of  $\alpha$  does not affect much the convergence rate, nor the stiffness of the jump. The jump is still very stiff (1-2 grid steps). However, it is clear that small values of  $\alpha$  lead to unacceptable oscillations. The profile decreases strongly ahead of the physical jump:  $h$  is as low as 0.35 m for  $Fr_1 = 10$  and  $\alpha = 0.6$ .

While most calculations have started from a sinusoidal initial profile, the run RSW1-17 was repeated as run RSW1-18 starting from a linear initial profile (Fig.7). The computation reveals the same convergence rate (Fig.8) and the final results are indistinguishable when plotted.

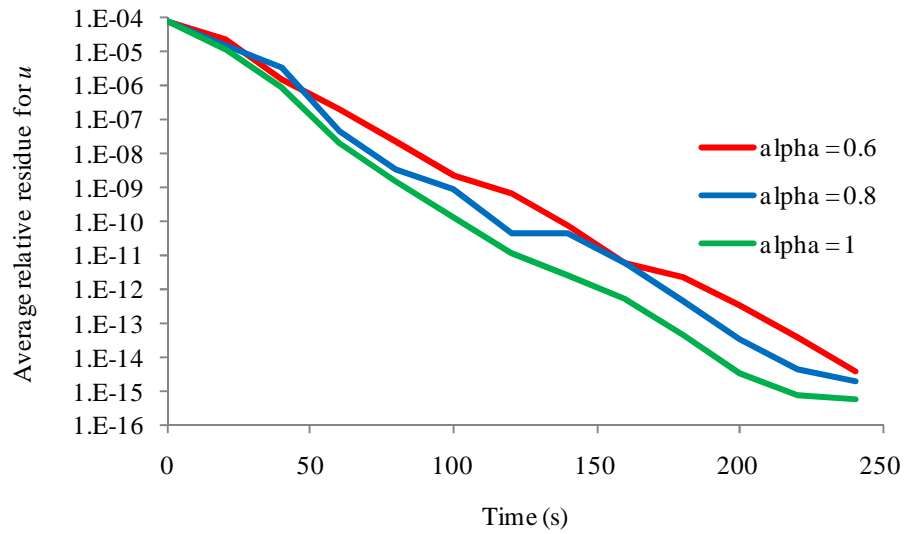


Fig.5: Convergence history for Fr<sub>1</sub> = 10 (RSW1)

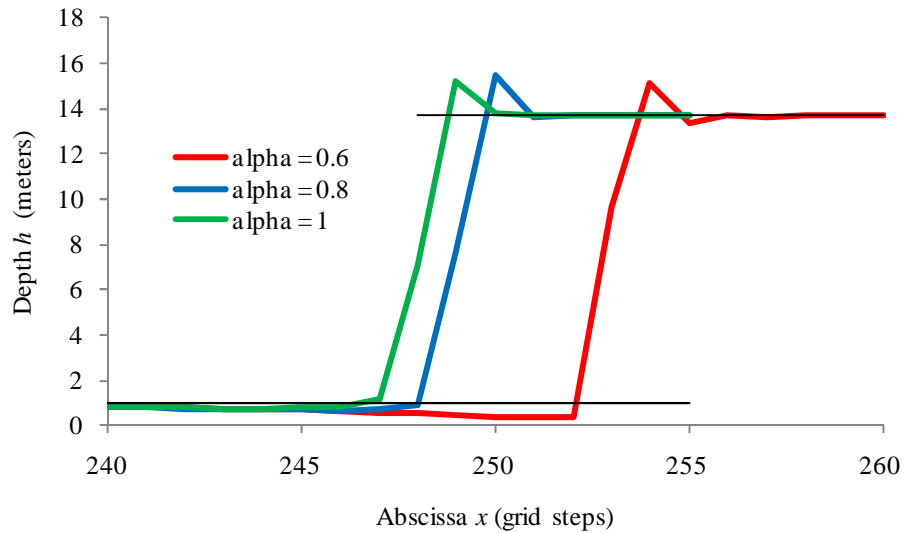


Fig.6: Distribution of depth  $h$  for Fr<sub>1</sub> = 10 (RSW1)

As explained in section 3, the NS-like terms can be kept as regularizing terms, as was done in the calculations presented above. Because the regularization has a somewhat arbitrary character, run RSW1-17 was repeated as run RSW1-19, with the NS-like terms removed. The term  $\frac{4}{3} \mu \frac{\partial u}{\partial x}$  was removed from  $\Pi$  in Eq.(18), which results in the coefficient 5/3 replaced by 1 in Eq.(21). The convergence is much slower (Fig.9). However, the final profiles are very similar (Fig.10) if we remember that the profiles can be translated arbitrarily along the  $x$ -axis.

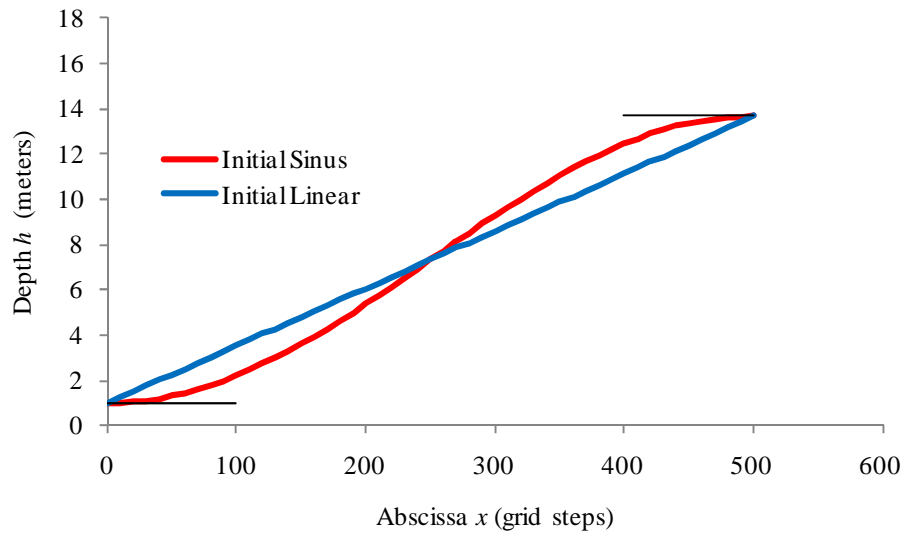


Fig.7: Initial profiles for  $Fr_1 = 10$  (RSW1)

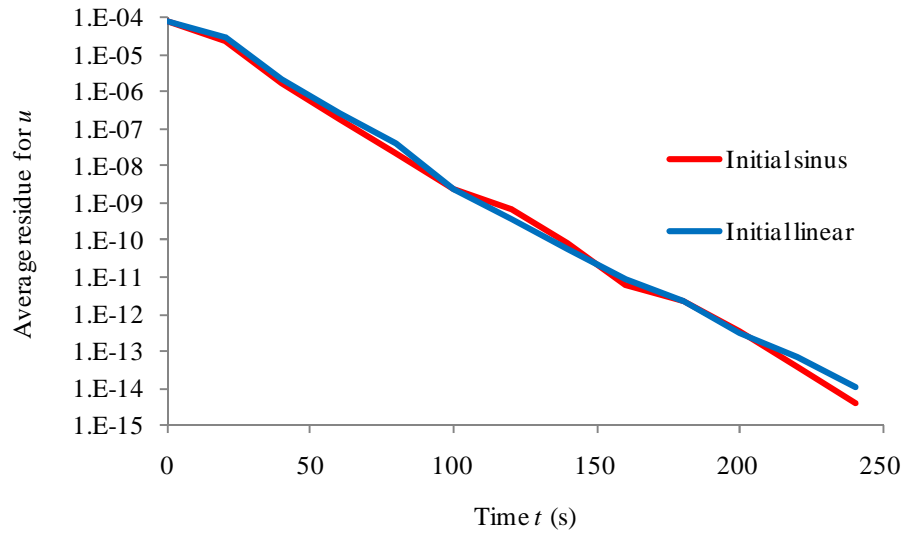


Fig.8: Convergence history for  $Fr_1 = 10$ ,  $\alpha = 0.6$  (RSW1, influence of initial profiles)

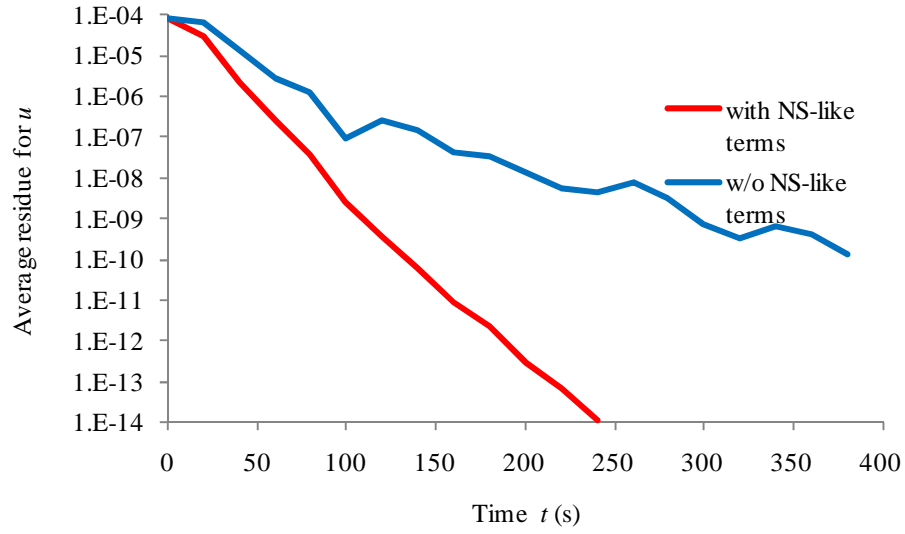


Fig.9: Convergence history for  $Fr_1 = 10$ ,  $\alpha = 0.6$  (RSW1, influence of NS-like regularizing terms)

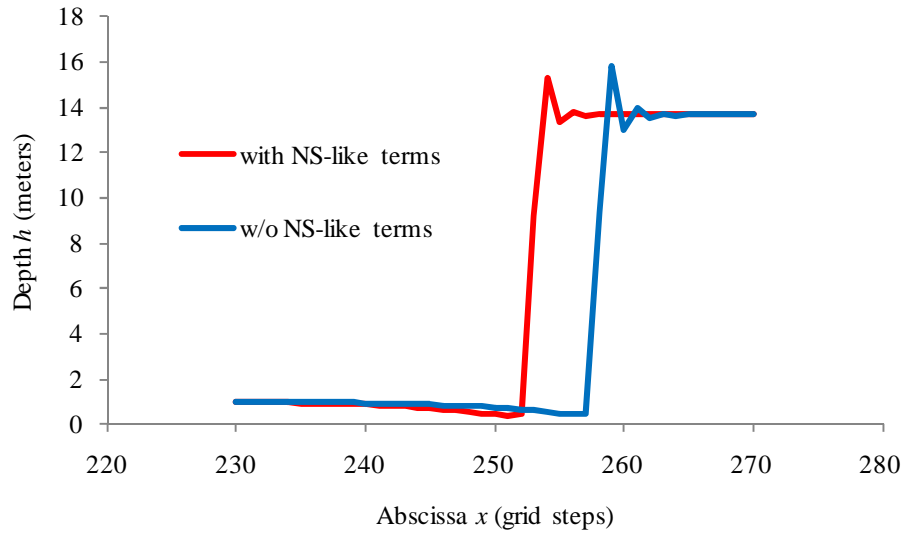


Fig.10: Distribution of depth  $h$  for  $Fr_1 = 10$ ,  $\alpha = 0.6$  (RSW1, influence of NS-like regularizing terms)

#### 4.4 Results for RSW2

A similar approach was applied to the second variant of RSW equations (RSW2). The initial conditions were characterized by a linear variation of  $h$  from  $h_1$  at input to  $h_2$  at output and the corresponding value  $u = (h_1 u_1) / h$ .

The conditions used for the different runs are summarized in Table 2. For a given Froude number and a given  $\alpha$ , different runs with increasing values of  $\beta$  were computed until divergence. The highest acceptable value of  $\beta$  was retained. The corresponding lines appear in bold in the tables.

The first case considered was characterized by

$$Fr_1 = 1.1, h_1 = 1\text{m}, u_1 = 3.445\text{m/s}, h_2 = 1.134\text{m}, u_2 = 3.038\text{m/s}.$$

The convergence history and the spatial distribution of depth  $h$  are plotted in Figs.11 and 12, respectively.

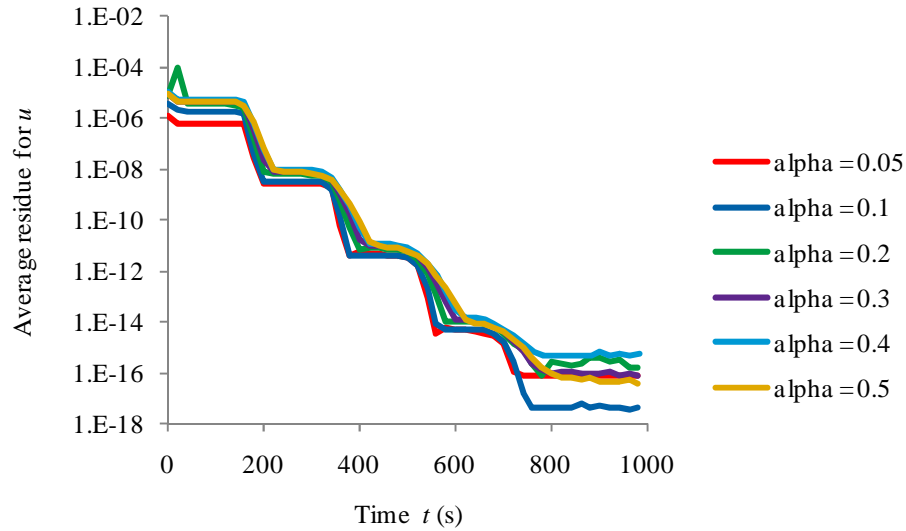
Increasing  $\alpha$  from 0.05 to 0.5 reduces the oscillations of the solution and simultaneously thickens the jump (Fig.12). This increases the stability of the equation system and allows increasing  $\beta$  and reducing the computing time. However increasing  $\alpha$  beyond 0.4-0.5 does not allow a further increase of  $\beta$ .

The run RSW2-09 was obtained with the same parameters as run RSW2-05, except that the grid step was twice larger. The thickness of the jump was identical in terms of grid steps.

The length of the computational domain was much larger than the jump thickness and did not affect the final profile, when changed from 100 to 200 m.

run	$Fr_1$	$\alpha$	$\beta$	$\Delta t$ (s)	$t_{\max}$ (s)	$res_{\text{avg}}$	$res_{\text{max}}$	CPU (s)
<b>RSW2-01</b>	<b>1.1</b>	<b>0.05</b>	<b>0.05</b>	<b>3.00E-03</b>	<b>1000</b>	<b>7.8E-17</b>	<b>1.5E-14</b>	<b>30.6</b>
RSW2-03	1.1	0.10	0.10	6.00E-03	1000	3.0E-17	1.1E-14	14.4
<b>RSW2-04</b>	<b>1.1</b>	<b>0.10</b>	<b>0.15</b>	<b>9.00E-03</b>	<b>1000</b>	<b>4.1E-18</b>	<b>1.4E-15</b>	<b>10.3</b>
<b>RSW2-05</b>	<b>1.1</b>	<b>0.20</b>	<b>0.30</b>	<b>1.80E-02</b>	<b>1000</b>	<b>2.9E-16</b>	<b>3.7E-15</b>	<b>5.3</b>
<b>RSW2-06</b>	<b>1.1</b>	<b>0.30</b>	<b>0.40</b>	<b>2.40E-02</b>	<b>1000</b>	<b>5.6E-17</b>	<b>2.3E-15</b>	<b>4.0</b>
<b>RSW2-07</b>	<b>1.1</b>	<b>0.40</b>	<b>0.50</b>	<b>3.00E-02</b>	<b>1000</b>	<b>5.7E-16</b>	<b>3.9E-15</b>	<b>3.2</b>
<b>RSW2-08</b>	<b>1.1</b>	<b>0.50</b>	<b>0.40</b>	<b>2.40E-02</b>	<b>1000</b>	<b>5.3E-17</b>	<b>1.1E-15</b>	<b>4.0</b>
RSW1-09	1.1	0.20	0.30	3.60E-02	1000	6.0E-17	1.2E-15	1.7
<b>RSW2-16</b>	<b>2.0</b>	<b>0.50</b>	<b>0.20</b>	<b>8.29E-03</b>	<b>250</b>	<b>2.4E-17</b>	<b>1.7E-15</b>	<b>2.7</b>
<b>RSW2-14</b>	<b>2.0</b>	<b>0.80</b>	<b>0.10</b>	<b>4.15E-03</b>	<b>250</b>	<b>1.3E-17</b>	<b>2.1E-15</b>	<b>5.5</b>
<b>RSW2-13</b>	<b>2.0</b>	<b>1.00</b>	<b>0.10</b>	<b>4.15E-03</b>	<b>250</b>	<b>2.8E-17</b>	<b>5.4E-15</b>	<b>5.4</b>
<b>RSW2-17</b>	<b>2.5</b>	<b>1.00</b>	<b>0.05</b>	<b>1.82E-03</b>	<b>500</b>	<b>2.0E-17</b>	<b>5.2E-15</b>	<b>23.8</b>

Table 2: Summary of runs with RSW2

Fig.11: Convergence history for  $Fr_1 = 1.1$  (RSW2)

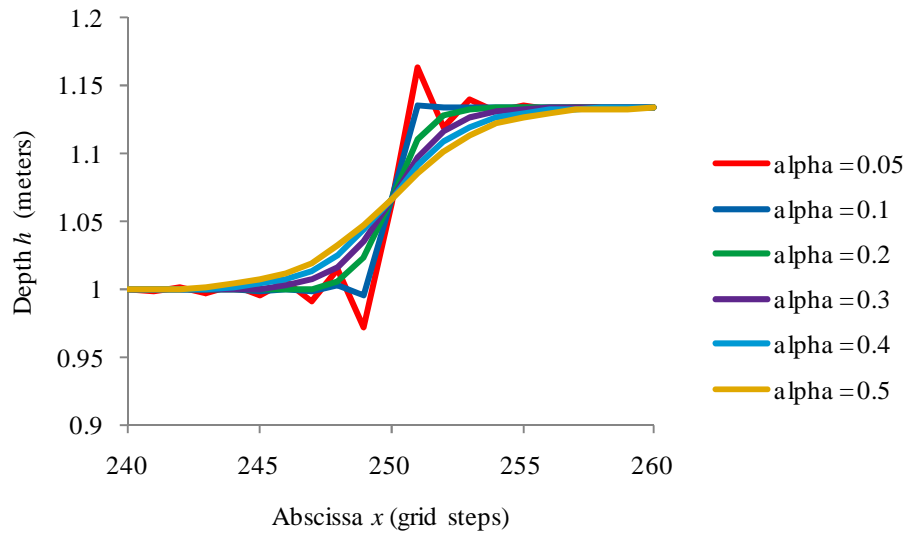


Fig.12: Distribution of depth  $h$  for  $Fr_1 = 1.1$  (RSW2)

A similar set of calculations was carried out for

$$Fr_1 = 2, h_1 = 1\text{ m}, u_1 = 6.264\text{ m/s}, h_2 = 2.372\text{ m}, u_2 = 2.641\text{ m/s}.$$

Convergence could not be obtained for  $\alpha < 0.5$ . Only the highest acceptable value of  $\beta$  is indicated in Table 2.

Finally, a hydraulic jump with

$$Fr_1 = 2.5, h_1 = 1\text{ m}, u_1 = 7.830\text{ m/s}, h_2 = 3.071\text{ m}, u_2 = 2.550\text{ m/s}$$

was also calculated. Only one set of parameters ( $\alpha = 1, \beta = 0.05$ ) resulted in a converged result.

For  $Fr_1 = 3$ , no combination of parameters ( $\alpha, \beta$ ) could be found to ensure convergence.

The maximal admissible value of  $\beta$  to be used when computing a hydraulic jump with the RSW2 equations is plotted in Fig.13 as a function of  $\alpha$  and  $Fr_1$ . As already mentioned before and also observed for RSW1 (Fig.2), increasing  $\alpha$  beyond 0.5 does not allow increasing  $\beta$  and there is no gain in terms of computing time.

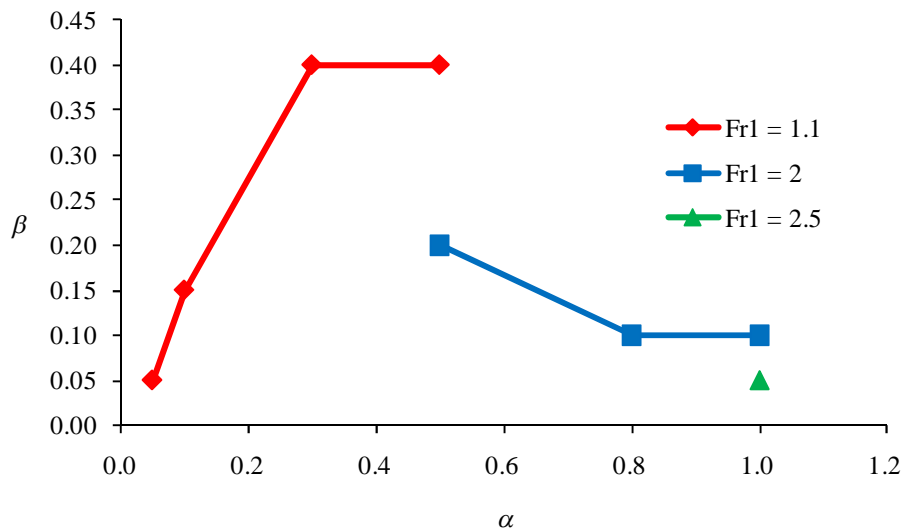


Fig.13: Maximal admissible value of  $\beta$  as a function of  $\alpha$  and  $Fr_1$  (RSW1)

## 5 CONCLUSION

The shallow water equations have been completed by regularization terms derived from additional terms contained in the *Quasi-GasDynamic* (QGD) and *Quasi-HydroDynamic* (QHD) equations. Although developed for gases, these terms could be applied to a liquid flow by considering the formal analogy between Euler equations and shallow water equations. Two variants of the resulting *Regularized Shallow Water* (RSW) equations were presented: RSW1 based on QGD terms and RSW2 based on QHD terms.

The regularizing terms involve an adjustable parameter  $\alpha$ . Increasing  $\alpha$  increases the stability of the system and allows the RSW equations being solved with a simple numerical algorithm, rather than by high-order numerical schemes as in [11, 12].

RSW equations have been applied to a test-case consisting in a hydraulic jump, characterized by its upstream Froude number  $Fr_1$ . A parametric study has been carried out on this test-case. The analytic solution served as a reference.

The computational time step is governed by the Courant parameter  $\beta$ . The maximum admissible value of  $\beta$  depends on  $Fr_1$  and on  $\alpha$ . Although the additional terms improve the stability of the system, increasing  $\alpha$  beyond 0.4-0.5 does not allow increasing further the time step.

Hydraulic jumps with  $Fr_1$  as high as 10 could be solved efficiently with RSW1 equations. The limits of the acceptable  $(\alpha, \beta)$  domain have been indicated.

RSW2 equations have a smaller domain of application. No acceptable combination of  $(\alpha, \beta)$  could be found for upstream Froude numbers larger than 2.5.

The additional terms may include or not Navier-Stokes-like viscosity terms. The presence of these terms is favorable to the stability.

The presented equations are very simple in their algorithmic implementation. The system converges fast with decreasing the mesh step. RSW methods may be efficiently generalized for unstructured triangular grids and may be efficiently implemented in modern multiprocessor and multinuclear calculation modules.

They appear as promising tools for the simulation of flows in real natural conditions.

## ACKNOWLEDGMENT

This work has been supported by the *Fund for Fundamental Researches* of the Russian Academy of Science under reference 10-01-00136.

## REFERENCES

- [1] J.J. Stoker, Water waves, The Mathematical Theory with Applications, *Interscience, New York* (1957)
- [2] L.D. Landau and E.M. Lifshitz, Hydrodynamics, *Nauka, Moscow*, (1986) [in Russian]
- [3] T.G. Elizarova, Quasi-Gas Dynamic equations, *Springer* (2009)
- [4] T.G. Elizarova, A.A. Khokhlov and Yu.V. Sheretov, Quasi-gasdynamical numerical algorithm for gas flow simulations, *Intern. J. for Numer. Meth. in Fluids* **56**, pp.1209-1215 (2008)

- [5] Yu. V. Sheretov, Dynamics of the continuum media for spatial-time averaging, *Izevsk, Moscow* (2009) [in Russian]
- [6] T.G. Elizarova and E.V. Shil'nikov, Capabilities of a Quasi-Gasdynamical Algorithm as Applied to Inviscid Gas Flow Simulations, *Computational Mathematics and Mathematical Physics* **49**, pp. 549-566 (2009)
- [7] T.G. Elizarova and E.V. Shil'nikov, Numerical Analysis of a Quasi-Gasdynamical Algorithm as Applied to the Euler Equations, *Computational Mathematics and Mathematical Physics* **49**, pp. 1869-1884 (2009)
- [8] A.A. Zlotnik and B.N. Chetverushkin, Parabolicity of the Quasi-Gasdynamical System of Equations, its Hyperbolic Second-Order Modification, and the Stability of Small Perturbations for them, *Computational Mathematics and Mathematical Physics* **48**, pp.420-446 (2008)
- [9] A.A. Zlotnik, Energy Equalities and Estimates for Barotropic Quasi-Gasdynamical and Quasi-Hydrodynamic Systems of Equations, *Computational Mathematics and Mathematical Physics* **50**, pp.310-321 (2010)
- [10] T.G. Elizarova and M.V. Afanasieva, Regularized shallow water equations, *Moscow University Physics Bulletin* **65**, pp.13-16, Allerton Press, Inc. (2010)
- [11] A. Birman and J. Falcovit, Application of the GRP scheme to open channel flow equations, *Journal of Computational Physics* **222**, pp.131-154 (2007)
- [12] M. Ricchiuto, R. Abgrall and H. Deconinck, Application of conservative residual distribution schemes to the solution of the shallow water equations on unstructured meshes, *Journal of Computational Physics* **222**, pp.287-331 (2007)